Proceeding of the IEEE
International Conference on Robotics and Biomimetics
Dali, China, December 2019

Structural Design and Analysis of Seed Implantation Robot Based on Flexible Shaft Transmission

Yongde Zhang, Jiawei Zhao and Yifeng Hu
Intelligent Machine Institute
Harbin University of Science and Technology
Harbin, China,150080
zhangyd@hrbust.edu.cn

Sihao Zuo
Foshan Baikang Robot Technology Co. Ltd., Foshan
Guangdong Province, China, 528000
bk_robot@163.com

***Abstract* - Seed implantation therapy has become an inevitable trend in the treatment of cancer because of its strong targeting, less trauma, definite curative effect and no side effects. However, most of the current seed implantation procedures are manually operated by doctors, and the accuracy of seed implantation is low due to fatigue. To solve this problem, this paper designs and analyzes a seed implanted robot based on flexible shaft Transmission. The robot is composed of a pose adjustment mechanism and a seed implantation mechanism. The pose adjustment mechanism is responsible for adjusting the pose of the seed implantation mechanism, the seed implantation mechanism is responsible for driving the horizontal movement of the hollow needle and the solid needle. The kinematics equation of the robot is obtained by kinematics analysis, and then the Monte Carlo method is used to simulate and analyze the workspace, which verifies the reliability of the design. Through the experimental analysis of the efficiency of the flexible shaft transmission, the influence of bending angle and load on it is obtained, which provides a good experimental basis for precise control.**

***Index Terms* - Seed implantation; Joint robot; Flexible shaft transmission; Kinematics analysis; Monte Carlo method.**

I. INTRODUCTION

Nowadays, with the development of society, people's living standards have improved significantly. In addition to solving the problem of food and clothing, more and more people are paying attention to their own health problems. The relevant data show that there are 18078957 new cancer cases in the world in 2018, the incidence rate is 236.9/ 100000, and the standardized incidence rate of the world standard population is 197.9/100000. 9555027 cancer deaths with a mortality rate of 125.2/100000 and a world standard population standardized mortality rate of 101.1/ 100000. It can be seen that cancer has become a major problem for people in the world [1].

Seed implantation therapy is to implant iodine 125 radioactive seeds into the diseased area and kill cancer cells with the help of its radioactivity, so as to achieve the purpose of treatment. The structure of iodine 125 radioactive particles is shown in Fig 1. Seed implantation therapy is suitable for the treatment of cancer patients who are unable to operate and can not withstand radiotherapy and chemotherapy. it has important clinical significance for the failure of chemotherapy, unresectable surgery and reducing the size of the tumor [2]. Because of its strong targeting, less trauma, definite curative effect and small side effects, it has become an inevitable trend in the treatment of cancer at home and abroad.

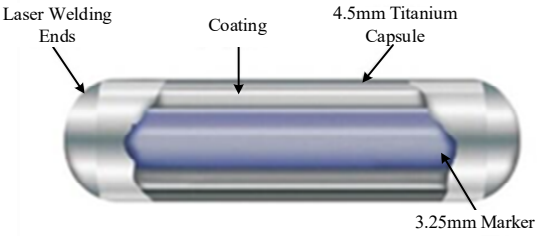

Fig. 1 Structure of iodine 125 radioactive seeds

Traditional seed implantation therapy uses a manual seed implantation device to implant seeds to the target point under image navigation such as MRI, TRUS or CT. General clinical surgery requires the implantation of 20 needles to place 80-120 seeds into the tumor area, which can cause doctor fatigue and can not continuously control the puncture force, resulting in the error of seed position [3]. The use of robot-assisted doctors to carry out seed implantation surgery can effectively solve this problem.

In recent years, the research of seed implantation robot has attracted the attention of scholars at home and abroad. Thomas Jefferson University has developed single channel Euclidian robot [4] and multi-channel MRIAB robot [5], Columbia University of Canada has developed UBC robot [6], Western Ontario University has developed RRI robot [7]. This kind of robot system has a large volume and is not suitable for flexible operation in a small space.The hybrid seed implantation robot has been developed by Tianjin University and Beijing Institute of Technology in China, which not only reduces the cumulative error accuracy of the robot, but also improves the motion flexibility, but it is only suitable for breast and cranio-maxillofacial tumor implantation. And the control is relatively complex [8,9].

In this study, a seed implantation robot based on flexible shaft transmission is designed, its kinematics and workspace analysis are carried out, and the factors affecting the flexible shaft transmission efficiency are analyzed by experiments.

II. STRUCTURAL DESIGN

The robot designed in this paper can not only complete the adjustment of the end pose, but also realize the autonomous implantation of seeds. The following is the discussion of the pose adjustment mechanism and the seed implant mechanism.

978-1-7281-6321-5/19//$31.00 ©2019 IEEE

A. *Pose adjustment mechanism*

For seed implantation robots, the pose adjustment mechanism needs to satisfy the following functions: rotary motion, horizontal motion and pitch motion; can work in a small or limited space; occupy less space and weight light and lower the center of gravity. In combination with the above functional requirements, consider the use of the mechanical arm structure for position adjustment.

The cartesian coordinate manipulator has high precision and easy control, but the overall structure has large size and poor flexibility. The spherical coordinate manipulator has a compact structure and a large working space, but its structure is relatively complex and its precision is not very high. The structure of cylindrical coordinate manipulator is simple and the overall size is small, but the accuracy is not very high. The structure of the swivel coordinate type manipulator is similar to that of the human arm, and its working range is large, the action is flexible, the structure is compact, and the floor space is small, but the subjectivity of motion is poor, and the control and operation are complicated. Through the comparison and analysis of the above mechanical arm scheme, combined with the required functions, it is decided to use the rotary coordinate type robot arm [10].

The rotary coordinate type manipulator is usually driven by the drive element at the joint, which will result in a heavier end and increase the load on the lower drive element. In order to solve such a problem, a parallelogram mechanism is designed in this paper to realize that the rotary driving element is located at the lower portion of the robot, which reduces the overall center of gravity and reduces the weight of the end. Since most of the seed implantation robots are used in a relatively narrow space, the power transmission of the robot is realized by the flexible shaft remote transmission, and the flexible shaft transmission has a greater advantage in absorbing vibration, mitigating shock and storing energy [11].

B. *Seed implantation Mechanism*

For seed implantation robots, the seed implantation mechanism needs to satisfy the following functions: the hollow needle and the solid needle can be smoothly, accurately and quickly reach the specified position in the horizontal direction; the overall size is small and suitable for narrow spaces.

The mechanism for realizing the horizontal movement of the hollow needle and the solid needle includes a gear - rack transmission mechanism, a synchronous belt transmission mechanism and a ball screw transmission mechanism, wherein the gear-rack transmission mechanism has a large bearing capacity, a high transmission speed and a long transmission distance. However, in the short-distance transmission, due to the presence of the return error, the positioning accuracy is reduced, and the processing and installation requirements are high. If the processing and installation accuracy is poor, the transmission noise is large and the wear is large; The synchronous belt transmission mechanism has the advantages of smooth operation, low noise, low cost and can ease the impact vibration load, but if the pretightening force is not suitable, the phenomenon of tooth skipping is easy to appear, and its service life is short, so the equipment needs to be readjusted every time it is replaced; The ball screw transmission mechanism has the advantages of small thermal deformation, small friction, stable size, compact structure, convenient installation, high transmission efficiency, long service life and good synchronization performance, but its transmission distance is close and its speed is slow. Through the above analysis, combined with the functions required to achieve, it is decided to use the ball screw drive mechanism to achieve the horizontal movement of the hollow needle and the solid needle [12].

Due to the need to control the hollow needle and the solid needle respectively, two ball screws are needed. Considering the limitations of the overall size and space, the two screws are placed side by side and are guide rails to each other, thus eliminating the guide rail of the screw nut and reducing the overall size. As shown in Fig 2.

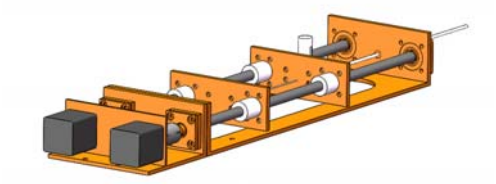

Fig. 2 Seed implant mechanism

The above designed structure is integrated and assembled to obtain an overall three-dimensional assembly drawing, as shown in Fig 3.

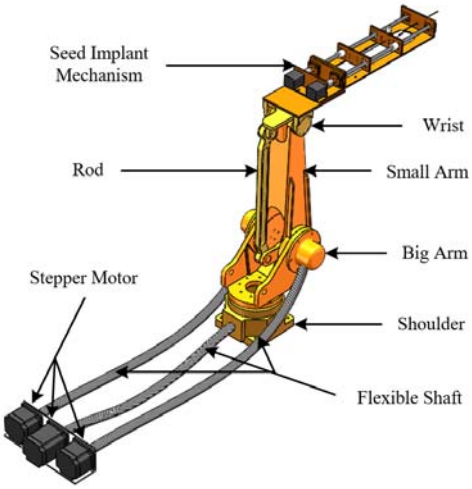

Fig. 3 Overall assembly drawing

III. STRUCTURAL ANALYSIS

A. *Kinematics analysis based on D-H method*

In order to describe the position and pose of the tip of the seed implantation mechanism in space, a coordinate system can be established on each joint, and the transformation relationship between the coordinate systems is used to describe the position of the needle tip pose [13]. The coordinate system is generally established by D-H method and the kinematic equation of the robot is derived.

The D-H method was proposed by Denavit and

Hartenberg in 1995 as a matrix method for establishing relative poses. It adopts a_n , α_n , d_n and θ_n four parameters to describe the relationship between the connecting rod itself and the adjacent connecting rod, so as to derive the equivalent homogeneous coordinate transformation matrix of the coordinate system of the end effector relative to the base coordinate system, thereby establishing the kinematics equation of the robot [14].

a_n and α_n are used to describe the parameters of the connecting rod itself, d_n and θ_n are used to describe the connection relationship between the adjacent connecting rods. The general formula for the change of the coordinate system between the two connecting rods is as follows:

$$^{i-1}\mathrm{A_i} = \mathrm{R_{z,\theta}T_{z,d}T_{x,\alpha}R_{x,\alpha}} = \begin{bmatrix} \cos\theta_i & -\cos\alpha_i\sin\theta_i & \sin\alpha_i\sin\theta_i & a_i\cos\theta_i \\ \sin\theta_i & \cos\alpha_i\cos\theta_i & -\sin\alpha_i\cos\theta_i & a_i\sin\theta_i \\ 0 & \sin\alpha_i & \cos\alpha_i & d_i \\ 0 & 0 & 0 & 1 \end{bmatrix} \tag{1}$$

In order to analyze the kinematics of the robot, it is necessary to establish the coordinate system. Therefore, simplify the above three-dimensional model into a connecting rod and establish a corresponding coordinate system [15], as shown in Fig 4.

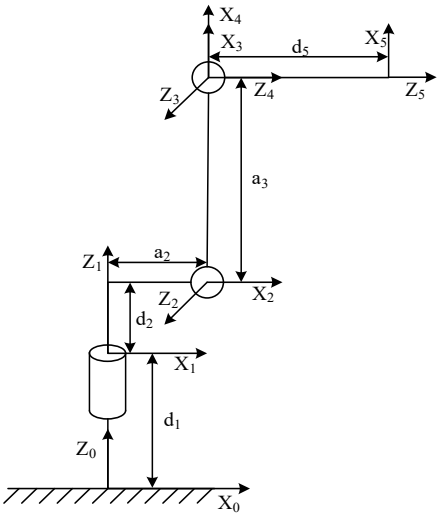

Fig. 4 Linkage coordinate system

The parameter list of the connecting rod D-H determined by the connecting rod coordinate system is shown in Table 1.

TABLE 1
D-H PARAMETER

link	variable	d	a	α	$\cos\alpha$	$\sin\alpha$
1	θ_1	d_1	0	0	1	0
2	θ_2	d_2	a_2	90°	0	1
3	θ_3	0	a_3	0	1	0
4	θ_4	0	0	90°	0	1
5	θ_5	d_5	0	0	1	0

According to the general formula (1) of the connecting rod coordinate system transformation and the D-H parameters in Table 1, the coordinate transformation matrix of the robot can be deduced.

$$^0A_1 = \begin{bmatrix} \cos\theta_1 & -\sin\theta_1 & 0 & 0 \\ \sin\theta_1 & \cos\theta_1 & 0 & 0 \\ 0 & 0 & 1 & \mathrm{d_1} \\ 0 & 0 & 0 & 1 \end{bmatrix} \tag{2}$$

$$^1A_2 = \begin{bmatrix} \cos\theta_2 & 0 & \sin\theta_2 & a_2\cos\theta_2 \\ \sin\theta_2 & 0 & -\cos\theta_2 & a_2\sin\theta_2 \\ 0 & 1 & 0 & d_2 \\ 0 & 0 & 0 & 1 \end{bmatrix} \tag{3}$$

$$^2A_3 = \begin{bmatrix} \cos\theta_3 & -\sin\theta_3 & 0 & a_3\cos\theta_3 \\ \sin\theta_3 & \cos\theta_3 & 0 & a_3\sin\theta_3 \\ 0 & 0 & 1 & 0 \\ 0 & 0 & 0 & 1 \end{bmatrix} \tag{4}$$

$$^3A_4 = \begin{bmatrix} \cos\theta_4 & 0 & \sin\theta_4 & 0 \\ \sin\theta_4 & 0 & -\cos\theta_4 & 0 \\ 0 & 1 & 0 & 0 \\ 0 & 0 & 0 & 1 \end{bmatrix} \tag{5}$$

$$^4A_5 = \begin{bmatrix} \cos\theta_5 & -\sin\theta_5 & 0 & 0 \\ \sin\theta_5 & \cos\theta_5 & 0 & 0 \\ 0 & 0 & 1 & d_5 \\ 0 & 0 & 0 & 1 \end{bmatrix} \tag{6}$$

Where: $^{n-1}A_n$ represents the coordinate transformation matrix from the $n-1$ joint to the n joint.

The reference coordinate system is set on the base surface, so the total coordinate transformation matrix from the base to the tip can be obtained by using the coordinate transformation matrix between the adjacent connecting rods. The calculation process and results are as follows:

$$^0A_6 = {}^0A_1{}^1A_2{}^2A_3{}^3A_4{}^4A_5 = \begin{bmatrix} n_x & o_x & a_x & p_x \\ n_y & o_y & a_y & p_y \\ n_z & o_z & a_z & p_z \\ 0 & 0 & 0 & 1 \end{bmatrix} \tag{7}$$

$$n_x = s_5(c_1s_2 + c_2s_1) + c_5[(c_3c_4 - s_3s_4)(c_1c_2 - s_1s_2)]$$
$$n_y = c_5[(c_3c_4 - s_3s_4)(c_1s_2 + c_2s_1)] - s(c_1c_2 - s_1s_2)$$
$$n_z = c_5(c_3s_4 + c_4s_3)$$
$$o_x = s_5[(s_3s_4 - c_3c_4)(c_1c_2 - s_1s_2)] + c_5(c_1s_2 + c_2s_1)$$
$$o_y = s_5[(s_3s_4 - c_3c_4)(c_1s_2 + c_2s_1)] - c_5(c_1c_2 - s_1s_2)$$
$$o_z = -s_5(c_3s_4 + c_4s_3)$$
$$a_x = (c_3s_4 + c_4s_3)(c_1c_2 - s_1s_2)$$
$$a_y = (c_3s_4 + c_4s_3)(c_1s_2 + c_2s_1)$$
$$a_z = s_3s_4 - c_3c_4$$
$$p_x = [d_5(c_3s_4 + c_4s_3) + (a_2 + a_3c_3)](c_1c_2 - s_1s_2)$$
$$p_y = [d_5(c_3s_4 + c_4s_3) + (a_2 + a_3c_3)](c_1s_2 + c_2s_1)$$
$$p_z = a_3s_3 + d_1 + d_2 - d_5(c_3c_4 - s_3s_4)$$

Where: $c_n = \cos\theta_n, s_n = \sin\theta_n$.

Let $P=\begin{bmatrix} p_x \\ p_y \\ p_z \end{bmatrix}$ be the pose transformation matrix of the robot, and the joint variables of each coordinate system shown in Fig 5,That is $\theta_1=0, \theta_2=0, \theta_3=90°, \theta_4=0$, $\theta_5=0$ bring in P can get the pose transformation matrix as:

$$P=\begin{bmatrix} a_2+d_5 \\ 0 \\ d_1+d_2+a_3 \end{bmatrix} \quad (8)$$

The resulting positional relationship is consistent with the position shown in Fig 5, indicating that the established kinematics equation is correct.

B. Workspace Analysis of Robots

The methods commonly used to solve the robot workspace are analytical method, graphic method and numerical method [16]. This paper uses the Monte Carlo method in the numerical method., which is a numerical method that uses random sampling to solve mathematical problems. The basic idea of applying this method to the robot workspace is that the joints of the robot work within a certain range of values. When all the joints are randomly traversed within their range of values, the set of all random values of the end points constitutes the working space of the robot.

Let the robot's workspace be $W(P)$, then the relationship between the pose transformation matrix and the workspace is:

$$W(P)=\begin{cases} p_x(\theta_n) \\ p_y(\theta_n) \\ p_z(\theta_n) \end{cases} \theta_n^{\min} \le \theta_n \le \theta_n^{\max}, n=1,2,\cdots,5 \quad (9)$$

Where, $\theta_n^{\min}$ and $\theta_n^{\max}$ respectively represent the lower and upper limits of joint motion, The relationship between p_x , p_y , p_z and θ_n has been found in the previous section. and will not be repeated here.

The work space $W(P)$ can be obtained by randomly taking θ_n a number of times within the range of values in which it is located, but since the amount of calculation is too large, it is necessary to perform operations by means of MATLAB. The basic idea is to use the $rand(j,1)$ function to generate N random values between 0 and 1 as random step variables $(\theta_n^{\max}-\theta_n^{\min})rand(j)$, $(j=1,2,\cdots,N)$, to obtain random joint variables as:

$$\theta_n=\theta_n^{\min}+(\theta_n^{\max}-\theta_n^{\min})rand(j,1) \quad (10)$$

Then the corresponding position point of the end point of the robot can be obtained by bringing θ_n into the workspace $W(P)$. The more the number of coordinate points, the more can reflect the actual workspace of the robot. Finally, the points that are sought are displayed by the point depiction method, and the point cloud image of the workspace of the robot is obtained, that is, the Monte Carlo workspace of the robot [17].

When using MATLAB for simulation calculation, the values of each parameter of the robot are as follows:

$\theta_1 \in [-\pi,\pi], \theta_2 \in \left[-\frac{\pi}{2},\frac{\pi}{2}\right], \theta_3 \in \left[-\frac{5}{12}\pi,\frac{1}{12}\pi\right]$,

$\theta_4=0$, $\theta_5=0, d_1=95mm, d_2=100mm$,

$a_2=90mm, a_3=350mm, d_5=460mm$,

The number of random coordinate points is $N=10000000$ .According to the obtained kinematics equation and the above parameters, the working point cloud map of the robot is obtained, as shown in Fig 5.

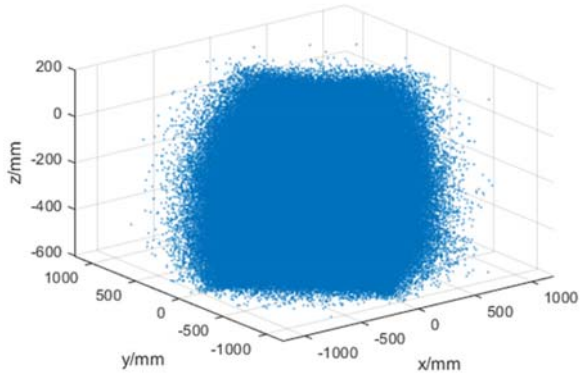

(a) Three-dimensional reachable space

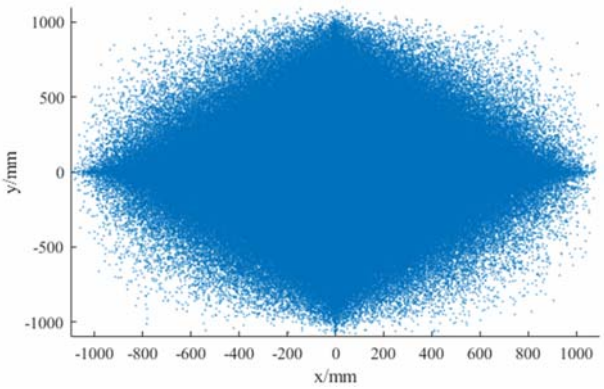

(b) XOY surface projection

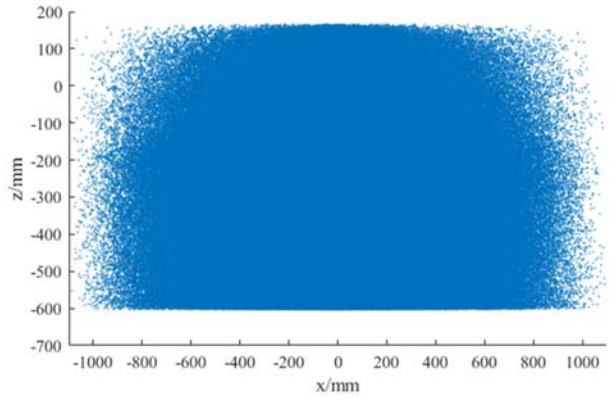

(C) XOZ surface projection

Fig. 5 Workspace point cloud map

It can be seen from Fig 6 that the accessible workspace of the robot is an approximate ellipsoid, whose workspace

range is roughly: $x \in [-1000, 1000] mm$, $y \in [-1000, 1000] mm, z \in [-600, 160] mm$, and enough to reach all parts of the human body. There is still some error between the point cloud map of workspace obtained by Monte Carlo method simulation and the actual workspace of the robot. Limited by the Monte Carlo method itself, the approximation degree of simulation results depends on the number of random Numbers. The more random Numbers obtained, the more coordinate Numbers calculated, and the more accurately the robot's workspace can be reflected.

IV. Experiment and Analysis of Flexible Shaft Transmission Efficiency

As a flexible transmission member, the flexible shaft inevitably loses a part of the power during long-distance transmission. This will cause the output rotation number of the motor to be different from the actually received number of revolutions, resulting in a significant drop in control accuracy. Therefore, studying the transmission efficiency of the flexible shaft is necessary to improve the accuracy. There are many factors affecting the efficiency of the flexible shaft transmission. Here we mainly study the influence of the bending angle of the load and the flexible shaft on the transmission efficiency of the flexible shaft [18].

The flexible shaft transmission efficiency is expressed as:

$$\eta = \frac{the\ input\ revolution\ number}{the\ output\ revolution\ number} \times 100\%,$$

where the input revolution number is the number of revolutions of the given motor of the computer, and the number of output revolutions is the number of revolutions measured by the encoder. The bending angle of the flexible shaft of this experiment is given as 0 degree; 30 degrees; 60 degrees; 90 degrees; 120 degrees, and the input and output are measured. The weight of the weight chip on the given load slider is 0kg; 1kg; 2.5kg respectively record the experimental data. A simplified model of the experiment is shown in Fig 6.

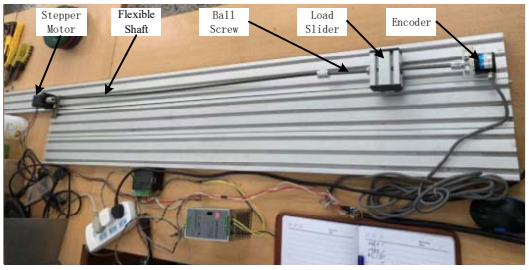

Fig.6 simplified experimental model

When the number of revolutions of a given motor is 10 laps, experimental tests are performed on different bending angles and different loads, and the following experimental data are obtained. The output angle after subtracting 3240° from the total output angle is shown in table 2, The Angle of loss through flexible shaft transmission is shown in table 3, and the transmission efficiency of flexible shaft is shown in table 4.

TABLE 2
Output Angle

	0kg	1kg	2.5kg
0°	359.25°	349.15°	348.375°
30°	354.825°	347.925°	346.875°
60°	352.425°	348.6°	341.1°
90°	351.15°	337.875°	336.95°
120°	346.2°	335°	332.475°

TABLE 3
Loss Angle

	0kg	1kg	2.5kg
0°	0.75°	10.85°	11.625°
30°	5.175°	12.075°	13.125°
60°	7.575°	11.4°	18.9°
90°	8.85°	22.125°	23.05°
120°	13.8°	25°	27.525°

TABLE 4
Transfer Efficiency

	0kg	1kg	2.5kg
0°	99.979%	99.699%	99.677%
30°	99.856%	99.665%	99.635%
60°	99.790%	99.683%	99.475%
90°	99.754%	99.385%	99.360%
120°	99.617%	99.306%	99.235%

In order to present the experimental data more intuitively, the experimental data in table 3 (Loss angle table) and table 4 (Transfer efficiency table) are drawn as line graphs by MATLAB, as shown in Fig 7 and Fig 8.

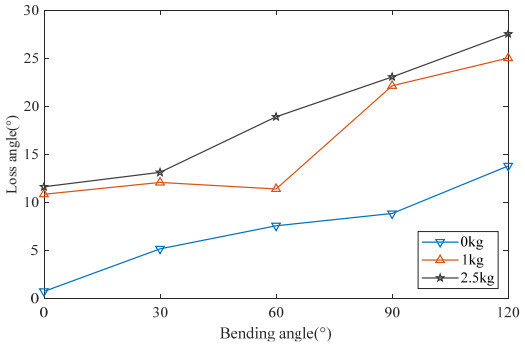

Fig.7 Loss angle

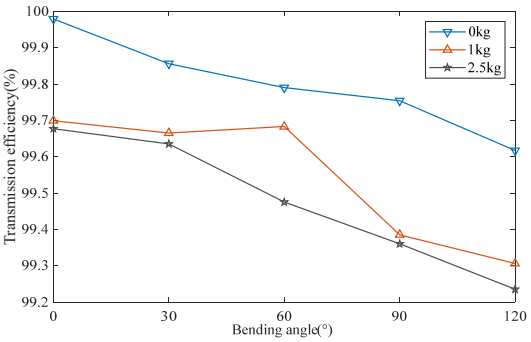

Fig.8 Transfer efficiency

The three broken lines in Fig 7 correspond to the relationship between the bending angle and the loss angle when the load is 0 kg, 1 kg and 2 kg, respectively. The three broken lines in Fig 8 correspond to the relationship between the bending angle and the transmission efficiency when the load is 0 kg, 1 kg and 2 kg, respectively. From Fig 7 and Fig 8, the following conclusions can be drawn:

(1) When the bending angle of the flexible shaft is the same, the larger the load, the larger the angle lost, and the lower the transmission efficiency.

(2) When the bending angle of the flexible shaft is the same, the loss angles when the load is 1kg and 2kg are not much different, but the loss angles when the load is 1kg and 2kg are different from the load when the load is 0kg.

(3) When the load of the flexible shaft is the same, the larger the bending angle, the larger the angle lost, and the lower the transmission efficiency.

(4) There may be a large error in the data when the bending angle is 60 degrees and the load is 1 kg.

According to the conclusions obtained from the above experiments, the transmission efficiency of the flexible shaft is related to the load and the bending angle, and it has a negative correlation trend. On the basis of this experiment, the seed implant robot designed in this paper can be used for multiple data acquisition and feedback training to compensate the error caused by the flexible shaft Transmission from the control angle to achieve more precise control.

V. CONCLUSION

Through the comparison of structure and function analysis, a 5-DOF seed implanted robot based on flexible shaft Transmission was designed. The kinematics equation of the robot is obtained by kinematics analysis, and then the Monte Carlo method is used to simulate and analyze the workspace, which verifies the reliability of the design. Through the experimental analysis of the efficiency of the flexible shaft transmission, the influence of bending angle and load on it is obtained, which provides a good experimental basis for precise control. The robot has a compact structure and a large working space, which basically meets the design requirements. However, the robots currently designed still have the disadvantages of slower needle insertion and less number of seeds carried at one time. The influential factors studied in the flexible shaft transmission efficiency experiment are relatively small, and the number of control experimental groups is relatively small. These problems will be further optimized and studied in the subsequent work.

REFERENCES

[1] Wang Ning, Liu Shuo, Yang Lei, et al. Interpretation of the 2018 Global Cancer Statistics Report [J].Journal of Multidisciplinary Cancer Management, 2019, 5(1): 87-97.

[2] A.Y. Liao, JJ.Wang,T.D.Wang,et al.Relative biological effectiveness and cell-killing efficacy of continuous low-dose-rate 1251 seeds on prostate carcinoma cells in vitro [J].Integrative Cancer therapies, 2010,9(1):59-66.

[3] N.Abolhassani Trajectory Planning and control of Needle Insertion in Robotics-Assisted Prostate Brachytherapy[D].London The University of Western Ontario,2008:45-74.

[4] YuY，Podder T，Zhang YD，et al.Robotic system for prostate brachytherapy[J].Computer Aided Surgery，2007，12（6）：366-370

[5] Podder TK，Buzurovic l，Huang K，et al.Multichannel robotic system for surgical procedures[C].In:Proceedings of the Imaging and Signal Processing in Healthcare and Technology Symposium，Was hington，DC，2011.737

[6] Salcudean S E , Prananta T D , Morris W J , et al. A robotic needle guide for prostate brachytherapy[C]// Robotics and Automation, 2008. ICRA 2008. IEEE International Conference on. IEEE, 2008.

[7] Wei Z，GardiL，Edirisinghe C，et al.Three-dimensional ultrasound guidance and robot assistance for prostate brachytherapy[M].Engineering Image-Guided Interventions ，Berlin:Springer-verlag，2008.429-460

[8] Jiang s，GuoJ，Liu S，et al.Kinematic analysis of a 5-DOF hybrid-driven MR compatible robot for minimally invasive prostatic interventions[J].Robotica，2012，30（7）：1147-1156

[9] Duan Xingguang, Chen Ningning, Wang Yongqian, Design and implementation of radioactive seeds implantation surgery robot for cranio-maxillofacial tumors [J], Mechanical Science and Technology for aerospace engineering, 201736 (3): 341346

[10] Liu Feng. Structural design and kinematic simulation of omnidirectional prostate biopsy robot [D]. Harbin University of Science and Technology, 2012.

[11] Chen Chang Da. Experimental study on the transmission characteristics of a novel flexible drive mechanism [D]. Beijing University of Posts and Telecommunications, 2018.

[12] Liang Yi. Research on key technologies of radioactive seed implantation robot for prostate [D]. Harbin University of Science and Technology, 2017.

[13] Zhang Yong De, Liang Yi, Bi Jinyu, Xu Yong. Kinematics modeling and simulation of seed implantation robot for prostate tumors[J]. Journal of Beijing University of Aeronautics and Astronautics,2016,42(04):662-668.

[14] Li Yazhen, Huang Jinying. Analysis of the forward kinematics and workspace of 8 － DOF manipulator[J].Journal of Mechanical Transmission,2016,40(04):94-96.

[15] Xu Cheng Yi, Li Yi Nong, Zhou Xiaoqing, Jiao En Zheng, Liu Ying. Kinematics analysis and simulation of MOTOMAN-UP6 robot[J]. Machine Tool & Hydraulics, 2013, 41(09): 144-149.

[16] Xie Fei Ya, Simulation of workspace of RPR robot based on MATLAB[J]. Value Engineering, 2017, 36(32): 116-117.

[17] He Yuanlai, Luo Jinliang, Pei Pengsong, Deng Jian. Workspace analysis of 7-DOF humanoid robotic arm based on monte carlo method[J]. Modular Machine Tool & Automatic Manufacturing Technique, 2015(03): 48-51.

[18] Zhang He Nan. Structure design and analysis of MRI-compatible robot based on flexible shaft transmission [D]. Harbin University of Science and Technology, 2016